Seismic array experiments to characterize tectonic tremor in the Anza gap, San Jacinto Fault

February 1, 2011 – January 31, 2012

United States Geological Survey

Award # G11AP20056

PI: Jean Paul Ampuero

California Institute of Technology

1200 E. California Blvd., MS 252-21

Pasadena, CA 91125

Phone: (626) 395-6958

Fax: (626) 564-0715

Email: ampuero@gps.caltech.edu

Seismic array experiments to characterize tectonic tremor in the Anza gap, San Jacinto fault

Final report

Introduction

Tectonic, or non-volcanic, tremor was first recognized and characterized in Japan in 2002 (*Obara*, 2002), and has subsequently been the target of extensive further study in Japan and elsewhere (see *Shelly et al*., 2006, and *Rubinstein et al.,* 2010, for recent reviews). Tectonic tremors are long duration, low amplitude seismic signals induced by natural sources, and are distinct from harmonic tremor associated with fluid migration that has long been observed in active volcanic settings (e.g., *Aki et al*., 1977). The signals generated by tectonic tremor are similar in many respects to those generated by cultural and non-tectonic natural sources such as traffic, wind, etc. The initial identification of tremor was based on the observation of noisy-looking transients correlated across a high-sensitivity seismic network (*Obara*, 2002). While the prolonged nature of tremor signals and absence of clear apparent phases complicated efforts to determine precise locations, later work identified so-called low-frequency earthquakes (LFEs) within tremor, i.e., events characterized by lower frequencies than tectonic earthquakes but with identifiable body-wave arrivals (e.g., *Shelly et al.,* 2006). Tremor is now thought to comprise LFEs, wholly or at least in part *(Shelly et al.,* 2006). Their low amplitude and swarmy nature is such that LFEs generally cannot be identified using standard seismic event detection methods, but rather require more sophisticated approaches such as autocorrelation and stacking of identified LFEs (e.g., *Ide et al.,* 2007; *Brown et al*., 2008).

Although a synoptic understanding of the underlying physical mechanism of tectonic tremor remains under development, results generally indicate that it is generated by shear slip on the plate interface, in or below the transition between a locked shallow zone and a creeping down-dip extension of the plate interface (e.g., *Ide et al.,* 2007). Tremor investigations have generated significant interest within the geophysical community because of the opportunity they offer to better understand the mechanics of fault systems and, potentially, the nature of earthquake nucleation and the earthquake cycle. Since 2002, investigations of high-quality seismic data has revealed that tremor occurs not only in Japan but also in other subduction zones, including Cascadia, Alaska, Costa Rica, and Taiwan (see *Rubinstein et al.,* 2010). Tremor triggered by dynamic strains associated with teleseismic waves has also been reported along some subduction zones, as well as in other regions (e.g., *Gomberg et al.*, 2008; *Peng and Chao*, 2008; *Peng et al.,* 2009; *Fry et al.,* 2011), including along the San Jacinto fault in southern California (*Wang et al*., 2013). Spontaneous tremor (i.e. not triggered by seismic waves) has been identified outside of subduction zones in only two regions, the San Andreas fault in central California (*Nadeau et al.,* 2005) and along a deep extension of the Alpine fault in New Zealand (*Wech et al*., 2012).

Identifying what controls the occurrence of tectonic tremors by comparing different source environments, and understanding their relation to other seismic and aseismic phenomena

has motivated attempts to detect tremor in other regions, including southern California. The San Jacinto fault has been an attractive target for investigation because of the reported presence of triggered tremor (*Gomberg et al.*, 2008; *Wang et al*., 2013), the presence of the dense Anza seismic network (*Berger et al*., 1984), its high rate of low- to moderate-magnitude seismicity (e.g., *Wesnousky*, 1994) and the expectation that a significant earthquake will occur in the future in the Anza gap (*Thatcher et al.,* 1975; *Sanders and Kanamori*, 1984). Furthermore, the hypothesized intermittent creep events in the lower half of the seismogenic zone near the Anza gap (*Wdowinski*, 2009) suggest the possibility of tremors generated by transient slow slip near the boundary between partially creeping and locked fault regions, by analogy to the tremor source region near Parkfield (e.g., *Shelly and Hardebeck*, 2010).

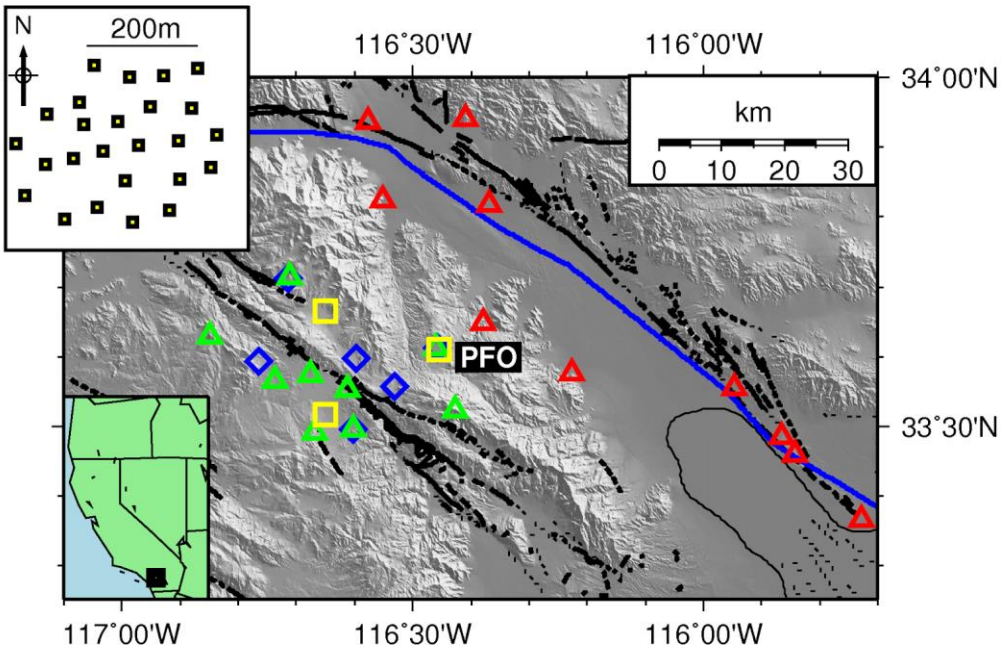

Figure 1. Map of the study area showing the seismic stations used in our analysis, including borehole instruments (blue diamonds) and broadband CISN stations in the Coachella Valley (red triangles) and in Anza (green triangles). Seismic arrays are shown in yellow. Mapped faults are shown in black, and the train tracks are shown in blue. The Coachella Valley spans the flat area crossed by the train. Inset map shows the configuration of the dense Pinyon Flat array, whose location is indicated by the label PFO. Truck traffic through the Coachella Valley primarily follows Interstate-10, which continues eastward into Arizona.

Here we report on properties of low amplitude transients detected by borehole seismometers near Anza that appear to be consistent in duration with tremor observed in other regions, but with a more peaked spectra between 3 and 4 Hz. To better understand the origin of these signals, we analyze data from a small--aperture array deployed in the Pinyon Flat Observatory in 2010 to explore the characteristics of identified transients,

given their ambiguous nature. We show that the results of these investigations point to a cultural rather than a geophysical source. The results suggest that noise sources are located within the Coachella Valley to the north/northeast/east of Anza, a major transportation corridor. We further explore the ambient noise wavefield by comparing data from borehole Anza stations with data recorded on surface stations within the Coachella Valley. We analyze both observed transients and the characteristics of background noise, and identify the key cultural sources that contribute to apparently noteworthy (quasi-harmonic and/or low-frequency) signals. Our results reveal that, if ambient tremor occurs on the San Jacinto fault, it is of low amplitude relative to cultural noise. These results provide a foundation for further efforts to identify tectonic tremor along the San Jacinto fault. We further show that, since the identified cultural noise sources probe depths intermediate to the depth ranges accessible to borehole and conventional seismic investigations, they provide a unique opportunity to refine the regional attenuation versus depth model.

Initial Identification of Transients in Anza Stations

Combining two established tremor detection techniques (*Obara*, 2002; *Brown et al.*, 2008), we analyze two years of continuous ground motion data (2008–2009) from 19 three-component seismometers in the target area. The composite network consists of 13 surface broadband stations from the California Integrated Seismic Network (CISN) and the Anza (AZ) seismic network, and six short-period sensors (2 Hz Geospace HS-1; see *Barbour and Agnew*, 2012) installed in boreholes as part of the Plate Boundary Observatory project (Figure 1). The algorithm involves two hierarchical stages, aiming first at transient detection and then at waveform decomposition into sequences of repeating signals. In the initial coarse detection stage we scan 20 or 30 minutes-long seismogram windows to identify periods of significantly increased energy in the 2-8 Hz frequency band that feature high similarity (high cross-correlation coefficient) of envelopes across four borehole stations (Figure 2). The corresponding seismograms are visually inspected to discard windows containing earthquakes or other obviously spurious signals and to assign a duration to each transient.

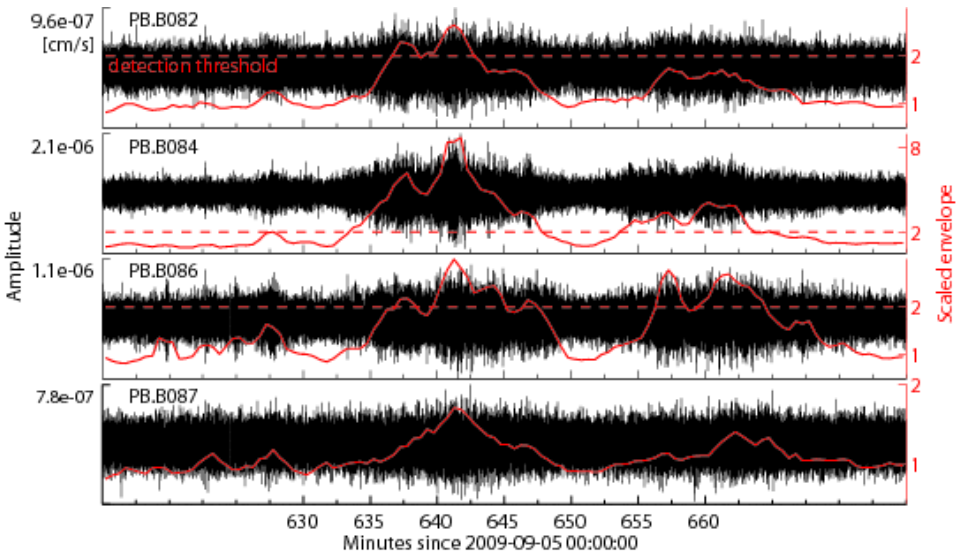

Figure 2. Seismograms (black, bandpass filtered from 2 to 8 Hz) during a transient identified by the initial coarse detection stage, based on a 30 minute correlation window. Station names are indicated in the top left corner. Detection is declared by three out of four borehole stations (the top ones). A detection is declared if the scaled envelope (red) raises for some time interval above the detection threshold (red dashed lines). Station PB.B087 is located to the west of the San Jacinto fault (Fig. 1). Envelopes are normalized by the envelope median in a window that includes the hour before and after the 30 minute search window. The threshold is set to two times this median estimate.

In the second waveform decomposition stage we scan the 57 available seismogram channels corresponding to coarsely detected time periods with the auto-correlation detection method of *Brown et al.* (2008), which attempts to decompose the signal into sequences of repeating patterns (Figure 3). We auto-correlate 6 s-long templates from the initially detected transients with the 24-hr long records of the same day. Compilation of individual clusters (lower parts of panels in Figure 3) are based on a high degree of waveform similarity across the 19 three-component stations. Similarity is measured from the cross-correlation coefficient, and clusters are assembled based on a dendrogram analysis. Finally, this 'weak' detection stage is extended by repeating the auto-correlation scan using waveform stacks (top parts of panels in Figure 3) which results in a catalog of 'robust' detections.

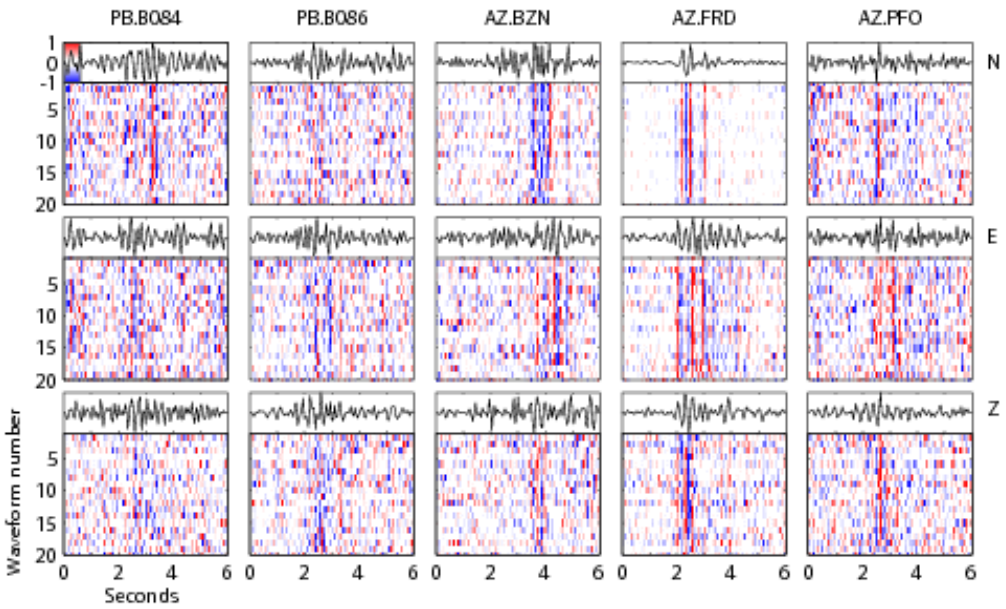

Figure 3. Decomposition of the large amplitude signal into sequences of repeating patterns. We show five three component clusters out of the total set of 19 stations. The lower parts of each panel show the individual waveforms that have been detected with the auto-correlation method of *Brown et al.* (2008). The seismograms on top are stacks of the lower data, and are used as master templates in an additional robust matched filter search.

We detect on average more than one transient per day (Figure 4). The rate of detected transients appears irregular, with several months-long periods of increased activity. Peak amplitudes of these transient signals observed in proximity to the San Jacinto fault are generally on the order of 10 nm/s (Figure 2), and are thus comparable to LFE amplitudes recorded on borehole stations near Parkfield (Figure 5b*; Shelly and Hardebeck*, 2010). On all stations the velocity spectra of the transients feature a peaked shape centered between 3 and 4 Hz (Figure 5), which is absent in recordings from earthquakes on the San Jacinto fault. This spectral characteristic contrasts with the spectral signature (within the 1-10 Hz band) typically reported for tremors; i.e., enriched in low frequency energy (*e.g, Shelly et al.,* 2007*; Ide et al., 2007; Wang et al.,* 2013), although some tremors near Parkfield show a similar spectral peak near 4 Hz (*Fletcher and Baker*, 2010).

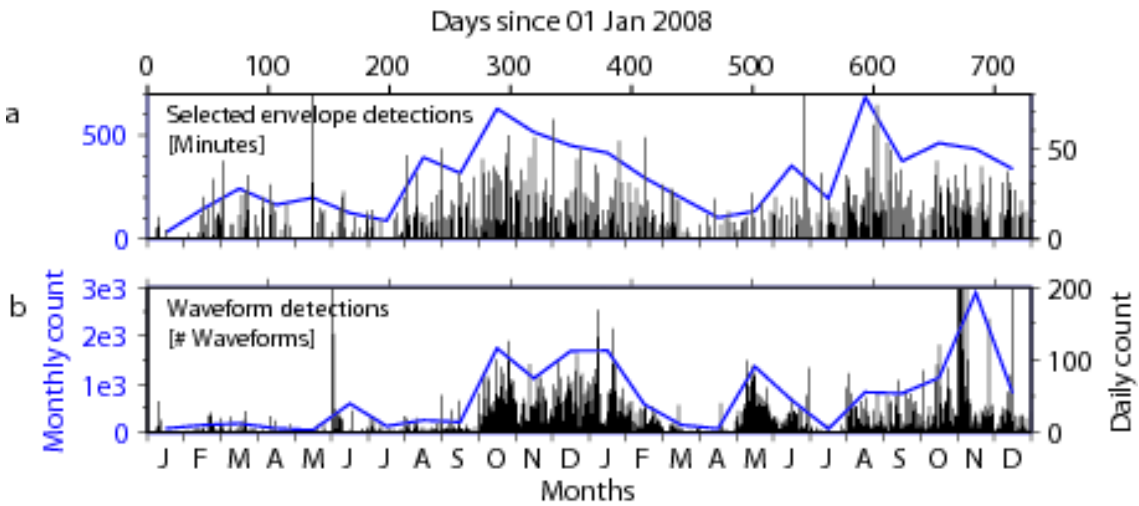

Figure 4. Detection statistics in the two stages of the tremor search procedure. (a) Cumulative transient duration from the initial coarse detection stage. (b) Number of individual 6-s waveforms identified by template auto-correlation.

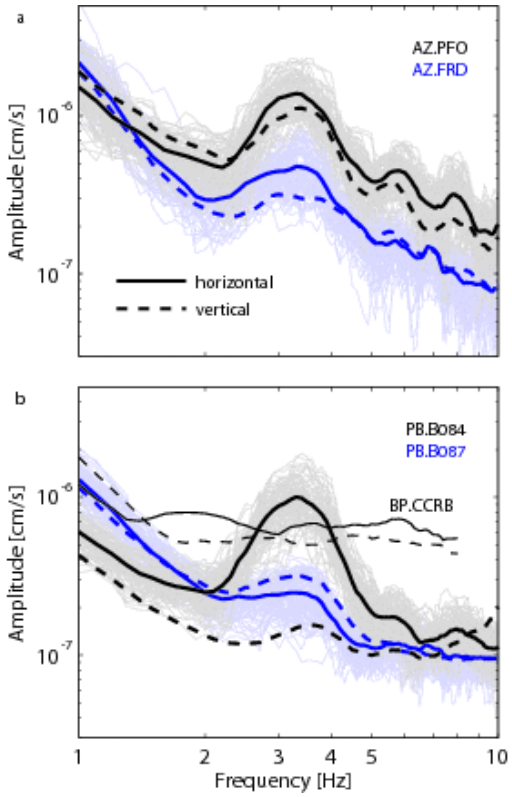

Figure 5. Velocity amplitude spectra of transients from two collocated borehole/surface station pairs (color coded; Fig. 1). (a) Surface stations. (b) Borehole stations. Grey and light blue lines are horizontal component spectra of consecutive 10-s windows taken from an 8-min-long transient (minutes 635-643 on 2009-09-05 in Figure 2). Heavy lines indicate 8-min averages. Thin black lines in (b) are tremor spectra from the San Andreas fault near Parkfield recorded at High-Resolution Seismic Network borehole station CCRB.

Dense Array Data and Results

To determine the source region(s) of the identified transients, we deployed a small-aperture array in Pinyon Flat Observatory, very close to stations AZ.PFO and PB.084 (see Figure 1). The array was operative between November 2010 and July 2011. Two other arrays were deployed in Anza for shorter periods (X weeks) between April-July, 2011. Each array consisted of 15-25 sensors with average spacing of about 60 meters. The array geometries were specifically designed to study signals with characteristic frequencies of 1-20 Hz. Equipment was provided by the IRIS PASSCAL Instrument Center. In this study we use the recordings from the Pinyon Flat array at which the transients are most clearly observed. We analyze the array data applying a coherency stacking technique (*Frankel et al, 1991; Fletcher et al*., 2006) to infer the ray parameters under the assumption of a single incoming plane wave. We focus on the transients identified during the deployment period using the same borehole stations and detection procedure described in the previous section. Data are filtered between 2 and 8 Hz, and the back-azimuth and apparent velocity are computed for 20 s windows with 50% overlap. Figure 6 shows the results of the analysis of a period containing four such transients. In the array data, these correspond to periods of increased amplitude (Figure 6a) and coherence (Figure 6b). They are characterized by a similar duration ~1000 s, a systematic temporal evolution of back-azimuth from near N to near NE, and an apparent velocity ~2500 m/s. Figure 7 shows a rose plot histogram of the back-azimuths estimated for the 100 strongest transients. The waves are consistently characterized by a N-NE-E back-azimuth. The array analysis also reveals a systematic temporal evolution of back-azimuth during each transient (Figure 6c), indicating sources that migrate in a consistent direction.

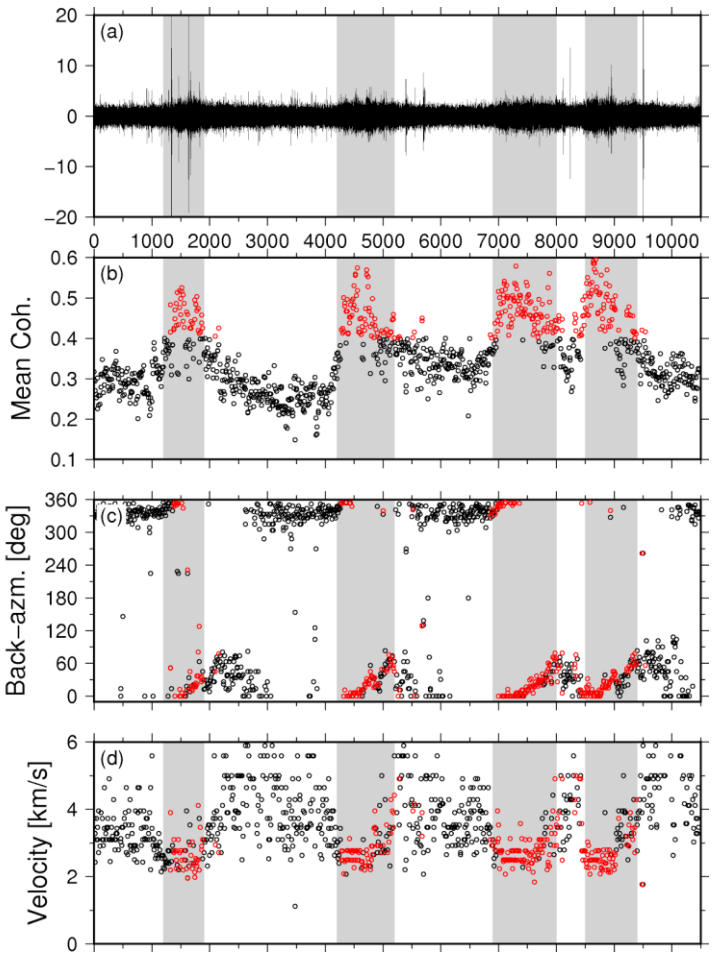

Figure 6. Train-induced ground motions recorded by a temporary seismic array in the Pinyon Flat Observatory. Time (in seconds) starts at 06:48:20 UTC on May 19th, 2011. (a) Ground velocity (μm/s) of the N-S component at one of the array sensors. Data are band-pass filtered between 2-8Hz. (b) The mean coherency, (c) back-azimuth and (d) apparent velocity of the array data. Grey windows indicate periods with strong train traffic noise. Red circles indicate estimates with mean coherency > 0.4.

Although large windmill farms operate in the Coachella Valley, they are primarily located to the N-NW of the back-azimuth range shown in Figure 7. Windmills would also not account for migrating sources. The results point to vehicle traffic noise, with back-azimuths pointing roughly in the direction of the nearest section of the railroad and highway I-10, the main traffic arteries along the Coachella Valley. Freight trains can be over 1 km long (from Google Maps snapshots and our own visual inspection), more than 100 times heavier than trucks and hence are the most obvious candidate source. As reported by the Federal Railroad Administration's Rail Crossing Locator mobile application, an average of 33 freight trains move daily through the Union Pacific Railroad in the northern Coachella Valley, between North Palm Spring and Mecca, at speeds typically slower than 70 mph and maximum speeds of 79 mph indicated from time tables. The speed limit for trucks in California is 55 mph; in practice typical speeds are likely to

be somewhat higher. Projecting the back-azimuths on the rail track or on the I-10 to estimate the velocity of the sources under the assumption that they are generated by trains or trucks, we find speeds of about 30 m/s (58 mph) consistent with the interpretation that the low-amplitude transients identified as potential tremor are in fact ground vibrations induced by vehicle traffic along the Coachella Valley.

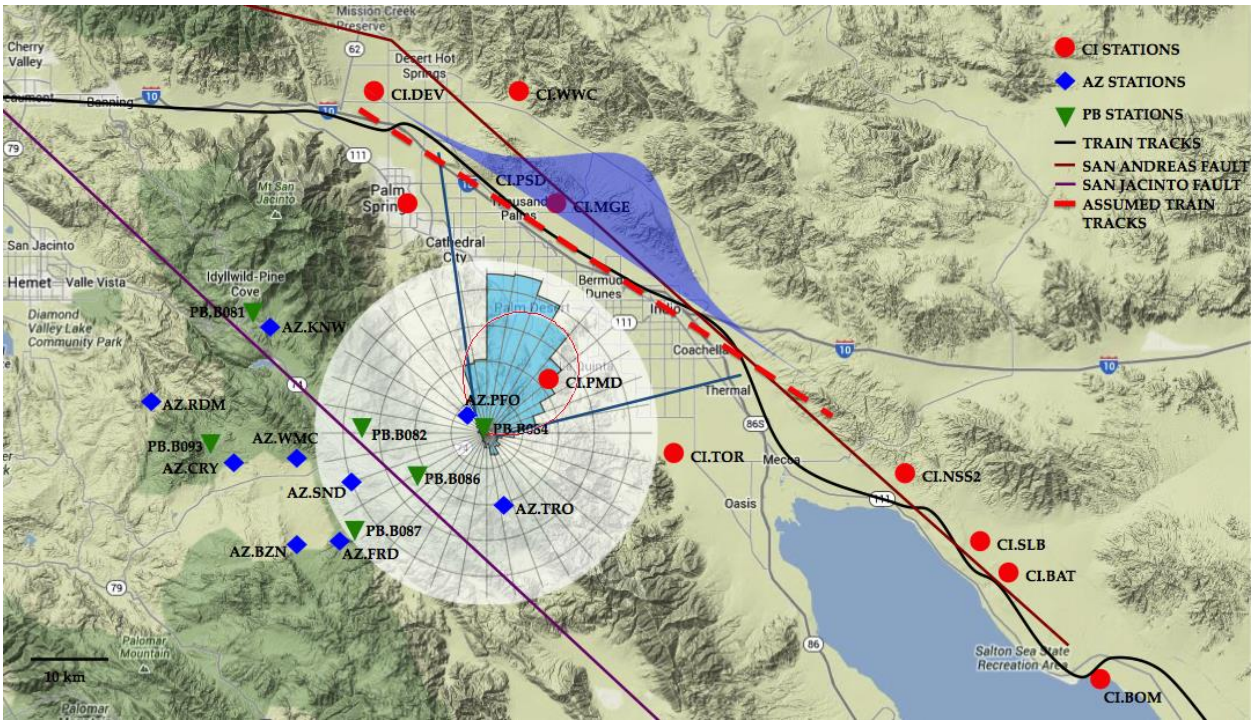

Figure 7. Map of the research area highlighting the borehole stations in Anza (green triangles) and some surface stations in the Coachella valley for reference (red circles). The histogram shows the back-azimuth of waves during the 100 strongest transients detected by a temporary seismic array in Pinyon Flats Observatory. The two blue lines emerging from the array indicate the portion of the railroad that is at a distance to station B084 closer than roughly 40 km, for which the predicted train noise amplitude is larger than the ambient noise amplitude at B084. The blue envelope in the vicinity of MGE is the wave amplitude predicted at Pinyon Flats Observatory as a function of train position along the railroad, assuming a straight railroad as indicated by the red dashed line. The red curve in the histogram shows this predicted relative amplitude as a function of azimuth.

Characteristics of Seismic Noise Induced by Trains

We next use surface stations in the Coachella Valley to investigate the nature and timing of signals generated by trains. Freight trains are privately contracted by Union Pacific and their schedules as well as their stops are proprietary. Additionally, passenger trains run along the same tracks at night following available schedules. Although the schedules for freight trains are not available, their induced ground vibrations are recorded by seismic stations near the tracks; thus the movement of all trains can be observed directly at CISN

sites (Figures 1, 7). We focus on data from 10 CISN stations at distances of roughly 1 to 10 km from the track (red circles in Figure 7). To visualize train noise we band-pass data between 2 and 8 Hz and plot time series along stations running from south to north. Figure 8 shows a record section corresponding to the period analyzed with array data in Figure 6. Four transients are clearly observed at station MGE, the CISN station nearest to where the track makes its closest approach to the Anza array. Their timing coincides with the timing of the transients identified from analysis of the PFO array data (Figure 6). The transients seen at MGE are also observed in the stations further south, with a systematic moveout that indicates source migration towards the south and is consistent with the back-azimuths measured at the PFO array. This confirms that the transients recorded at the PFO array are indeed generated by freight trains.

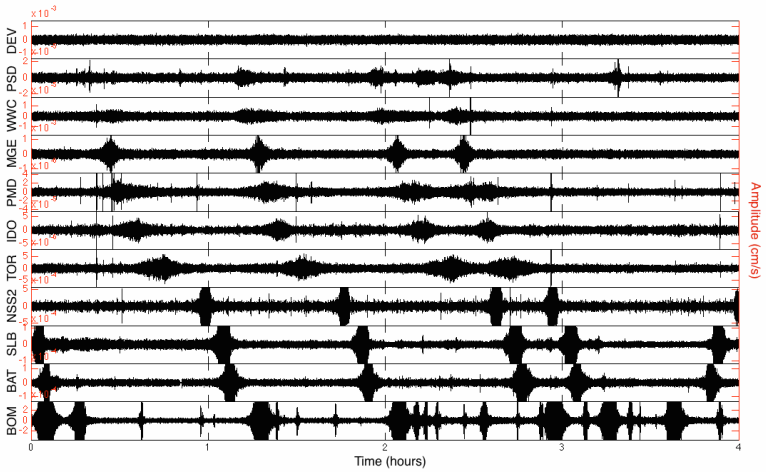

Figure 8: Time series (which component) for stations aligned from northwest to southeast along the Coachella Valley for the same period as in fig 6. Four trains running South.

Figure 9 shows another record section, 4 hours in length, in which the signature of trains traveling both south and north, with a crossing near MGE, is readily apparent. These record sections are typical of those observed from other times. From these plots we estimate a rough train speed of 12-21 m/s (27-47 mph). This is lower than the maximum train speed but consistent with expectations for average speeds.

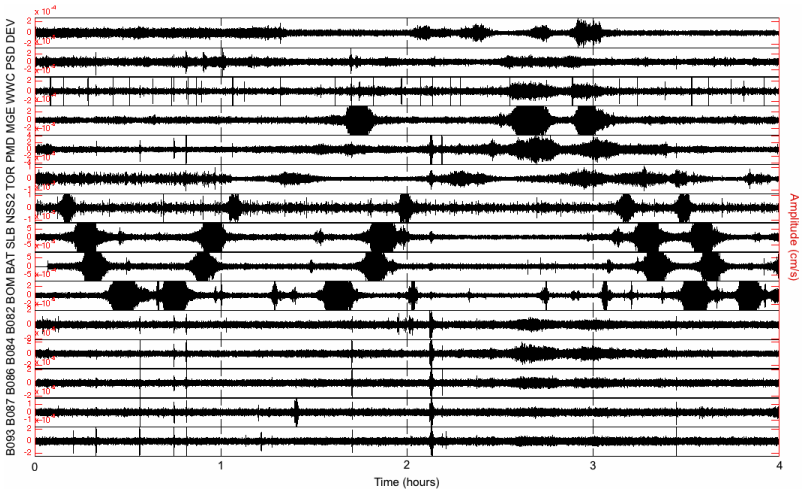

Figure 9. Train activity recorded by stations in the Coachella Valley from 8:00 to 12:00 UTC on 5 September 2009. Seismograms shown are north components band-pass filtered between 2 and 8 Hz, except for BAT where the vertical component is used. Each conspicuous transient corresponds to a train passing a station. The surface stations are ordered from north (top) to south (bottom). The especially large transient observed at station MGE around 2.5 hours corresponds to the passing of northbound and southbound trains. The vertical scale is set as the median absolute deviation of each seismogram multiplied by 40 for the top figure and 20 for the bottom one.

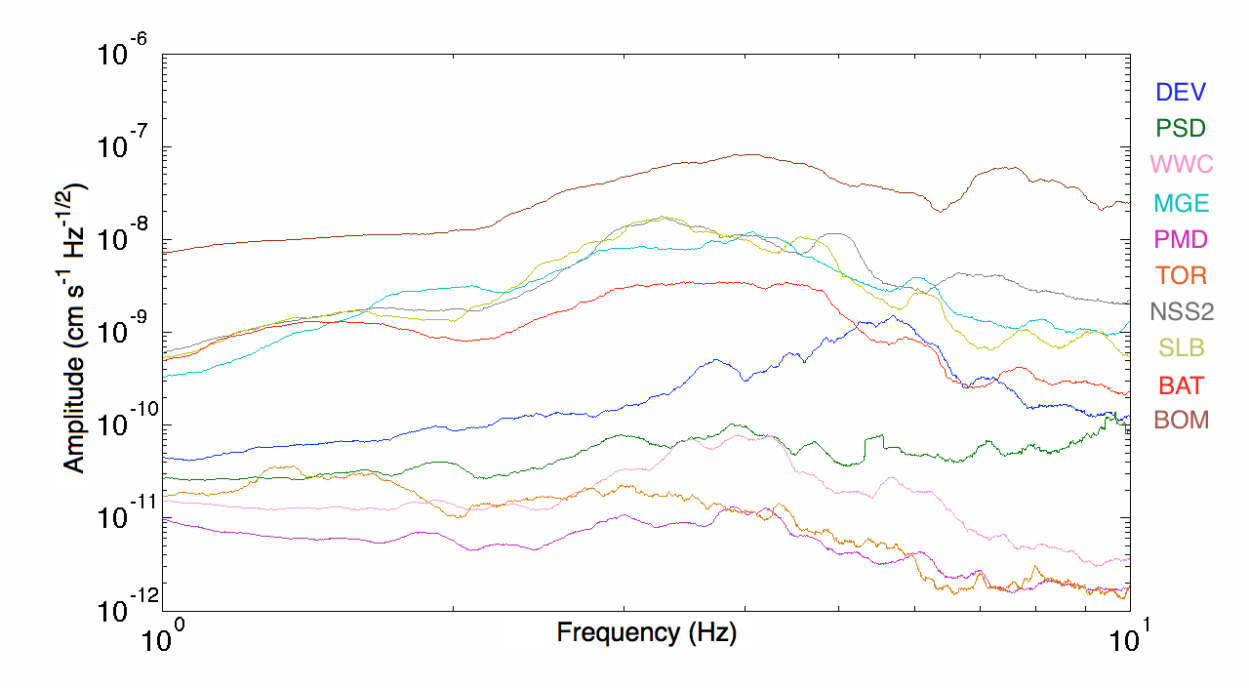

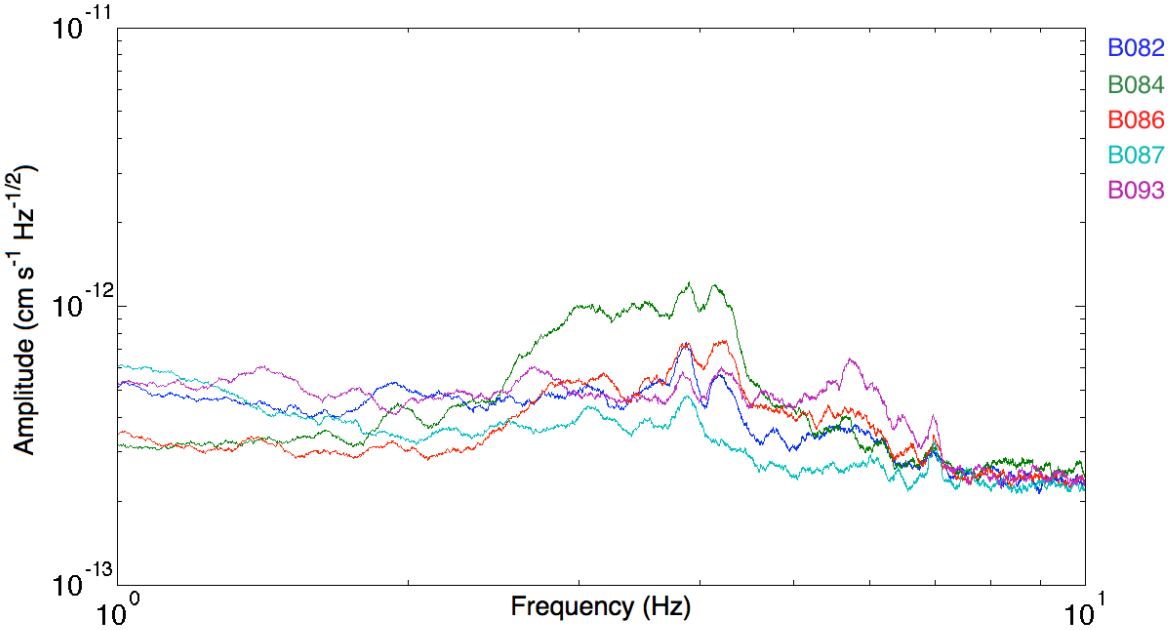

Figure 10. Spectra of ground motions induced by one of the trains passing on 5 September 2009 recorded by (a, top) surface stations in the Coachella valley (during time periods shown in the table below) and (b, bottom) borehole stations in the Anza region (for the interval 10:50:00-11:10:00 UTC). All signals were high-pass filtered over 0.1 Hz and a running smoothing window of 200 points was applied to the spectra.

Train passing by station	UTC time of pass-by
DEV	10:53:00-11:03:00
PSD	10:50:00-10:57:00
WWC	10:52:00-11:04:00
MGE	10:55:00-11:01:00
PMD	10:56:00-11:09:00
TOR	11:07:00-11:25:00
NSS2	11:27:00-11:32:00
SLB	11:34:00-11:38:00
BAT	11:37:00-11:40:00
BOM	11:48:00-11:51:00

We further consider the spectral signature of the transients observed in the Coachella

Valley using windows 6 minutes long centered on individual transients. This time duration is comparable to the typical transient duration. We smoothed spectra with a moving average over 200 sample points (~0.55 Hz width). The spectra are found to be peaked near 4 Hz (Figure 10a).

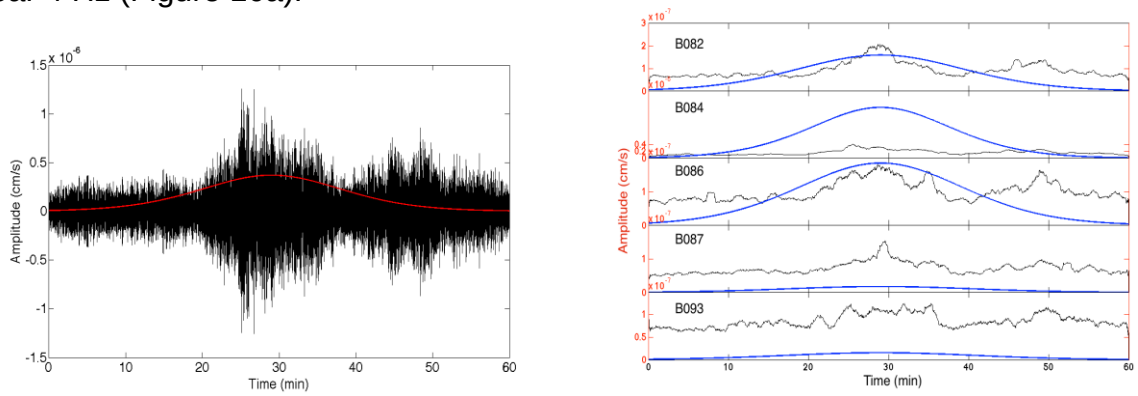

Figure 11. Transient at borehole station B084 (filtered between 3-4 Hz) at 10:12:00 on 05 Sep. 2009, associated with an identified train crossing near station MGE. The red line is the theoretical envelope of the transient as described in the text (note that equation 1 provides a predicted envelope shape, but not its overall amplitude).

We next consider the signals recorded by stations in the Anza region during periods of train traffic identified on stations in the Coachella Valley. We find that low-amplitude transients (with typical signal-to-noise ratio of 2 to 3) are observable on all the borehole stations in Anza by visual inspection of filtered seismograms (Figures 2 and 4). The only exception is station B093, which is the furthest away from the railroad. These transients are not visible on the surface stations, except at station PFO. The coarse detector based on envelope cross-correlation is sensitive to even weaker transients. Their typical duration is about 20 minutes and their timing generally corresponds to the times when trains are passing through the section of the rail track nearest to Anza. The spectra of the transients recorded at the borehole stations is peaked from 3 to 4 Hz (Figure 10b), not unlike the spectra of train-induced transients recorded in the Coachella Valley (Figure 10a). The borehole spectra are more strongly peaked than spectra observed in the Coachella Valley. This is consistent with expectations given the 2-Hz corner of the borehole instruments and the preferential attenuation of high frequencies along the path between the valley and Anza.

Freight Car Resonance

To test the hypothesis that trains generate the observed transients, we undertook reconnaissance fieldwork to measure directly the natural period of a freight train car. Modern freight train cars are connected to axles and wheels via a railroad truck, or bogie, which has a secondary suspension system. We observed the impulse response of a parked train car by jumping on it and measuring the vibrations with the built-in accelerometer of a cellular phone placed on its deck. We find a sharp peak around 3 Hz (Figure 13). Although these data were collected using a low-resolution instrument, visual inspection confirms a strong 3-Hz resonance, and shows that this response was

controlled by the secondary suspension system. It is expected that this resonance is controlled primarily by the overall size of the train as well as the gross characteristics of the suspension system. Thus it is not expected to vary significantly for different types of train cars.

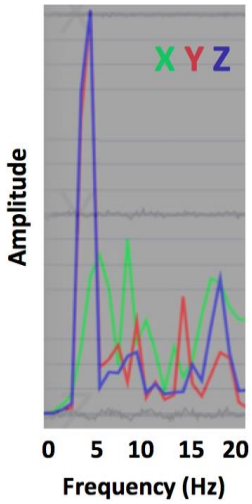

Figure 13. Spectra (arbitrary units) of freight train car vibrations induced by a human jump recorded by a mobile device. The X and Y components were roughly aligned with the width and length of the wagon.

Attenuation

We can further consider the amplitude of the transients seen on the borehole stations to estimate attenuation in the Anza region. Assuming the signals are high-frequency Rayleigh waves affected by attenuation, their amplitudes, Av, are predicted to decay as a function of distance, r, as

$$Av \propto e^{-\pi f r/VQ}/\sqrt{r} \qquad (1)$$

which is commonly written as

$$Av \propto e^{-\pi f t*}/\sqrt{r} \qquad (2)$$

where f is frequency, V is the wave velocity, Q the attenuation quality factor, and t* is an attenuation operator that *Anderson and Hough* (1984) equate to the observed spectral decay parameter kappa. Given depth-dependent Q and V, t* will be given by the integral of 1/VQ along the ray. As an approximation we assume a frequency-independent *Q*. Although attenuation is expected to be frequency-dependent between 1 and 10 Hz, it is reasonable to consider a frequency-independent Q given the narrow bandwidth of the signals. Considering the observed decay of the spectral amplitude at 3.5 Hz of transients detected at MGE as well as the borehole stations (Figure 6), we find that a Q value of 100 is roughly consistent with the observations across the borehole array. Previous studies have estimated local and regional attenuation at Anza. *Hough and Anderson* (1988) use data from surface Anza stations to estimate frequency-independent shear-wave Q values of approximately 500 in the upper ≈5 km. Using shallow logging techniques at surface

Anza stations KNW and PFO, *Fletcher et al.* (1990) estimate Q values of approximately 10 in the upper 50 m. The transients generated by trains have a predominant frequency of approximately 3 Hz; assuming a velocity of 3 km/s, that suggests a skin depth on the order of 500 m, intermediate between the two depth ranges for which attenuation has been estimated in previous studies.

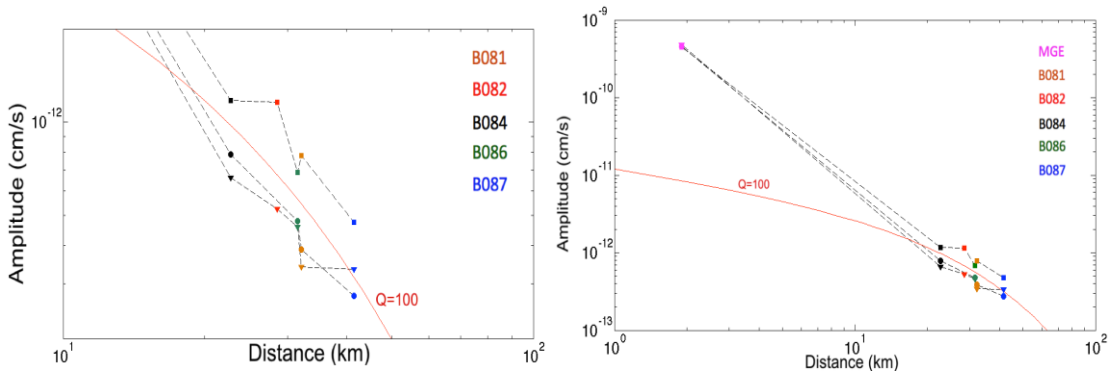

Figure 12. Spectral amplitude at 3.5 Hz observed at Anza borehole stations during train-induced transients, as a function of distance to the nearest point on the railroad. Three different events are shown (2008-10-26 19:02:00 +1800 s; 2009-09-05 10:30:00 +2400 s; 2009-11-22 08:30:00 +1800 s), indicated by symbol shapes and grouped through dashed lines. Stations are indicated by colors, as shown in the legend. The depth below surface of each station is indicated in the table below. The red lines indicate the expected decay of attenuated surface waves at 3.5 Hz, assuming a group velocity of 2.5 km/s and Q=100.

Station	Depth (meters)
CI.MGE	0
PB.B081	229
PB.B082	220
PB.B084	147
PB.B086	226
PB.B087	147

The Q value estimated in this study is an effective average path Q over the depth sampled by the presumed high-frequency surface waves. Since attenuation is estimated based on relative amplitudes at borehole stations, the value will not reflect attenuation within the upper 150-200m. Our result can be considered together with results for other depth

ranges to refine the Q(z) model in the Anza region. The results of *Fletcher et al.* (1990) indicate a t* estimate, 0.003-0.004s, for the upper 50 m at stations KNW and PFO. From analysis of seismic data one can estimate t* for the upper 5000 m from the observed spectra decay parameter, kappa, at zero epicentral distance, kappa(0) (e.g. *Anderson and Hough*, 1984). Values of kappa(0) at Anza are low in comparison to values observed at other sites in California, and are difficult to estimate precisely. *Campbell* (2009) estimates an average kappa(0) of 0.007 s for the six Anza sites where hard rock is encountered at relatively shallow depths. Thus, attenuation within the top 50 m accounts for approximately half of the attenuation within the uppermost 5 km. Our effective Q estimate of 100 implies that attenuation between 200-500 m will contribute a t* value of ≈0.0011 given velocity structure constrained from borehole and regional data (*Fletcher et al.*, 1990; *Yang et al*., 2012). Assuming Q=100 for depths between 50-200 m, the estimated t* contribution for 50-500 m is approximately 0.002 s. Attenuation between depths of 50-500 m is thus estimated to account for over half of the t* contribution from the top 50-5000 m. Thus, for depths between 500 and 5000 m, the contribution to t* is only approximately 0.0015 s, corresponding to Q~1000 given Vs=3000 m/s (e.g., *Yang et al.*, 2012). Although the calculations are simplified, they reveal that Q(z) structure at Anza increases more steeply with depth than suggested by the simple models inferred by *Anderson and Hough* (1988), which are sensitive only to integrated attenuation over the top 5 km.

The results of our attenuation analysis allow us to identify the stretch of the railroad where train traffic most efficiently generates noise seen on the Anza borehole stations. Making use of the calibrated amplitude-distance relation (equation 1) and assuming a single train running along the Coachella Valley railroad with speed $c = 17$ m/s, acting as a steady source of seismic waves, we can calculate a transient envelope shape at Anza. As a further simplification, we represent the segment of the railroad that lies nearest to station B084 as a straight line (roughly between stations DEV and NSS2, see the dashed red line in Figure 7). Essentially, we obtain a time-dependent signal amplitude $v(t)$ by setting $r = \sqrt{d^2 + (ct)^2}$ in equation 1, where $d = 25$ km is the nearest distance between B084 and the railroad and t is time relative to the passage of the train by the nearest point. The theoretical envelope is of comparable duration and envelope shape as the transients observed at the borehole stations (Figure 11). The results of the array analysis (Figure 7) suggest that dominant energy is generated along a section of track somewhat shorter than the extent of track delineated by the blue lines in Figure 7. We speculate that this might be due to either path effects, or to the fact that the train track departs from the assumed linear shape. Nonetheless, our results (Figure 11) demonstrate a good general agreement between the predicted and observed transient durations.

Characteristics of Seismic Noise Induced by Trucks

In addition to transients, we also identify a steady 3-4 Hz hum persisting for hours on many of the borehole instruments. Its amplitude is typically weaker by a factor of approximately 2 than that of the train-induced transients. The hum is seen on the same stations that record the transients, except for the surface station PFO (Figure 14).

While the hum and transients have a common spectral signature, there are too few trains running per hour through the nearest segment of the railroad to produce such a steady signal in Anza. Figure 14 shows the spectrogram at B084 including a period of about one hour over which trains were absent (corresponding to the first 7000 s in Figure 8), but the steady hum is still recorded. This example indicates that the hum is not associated with train activity.

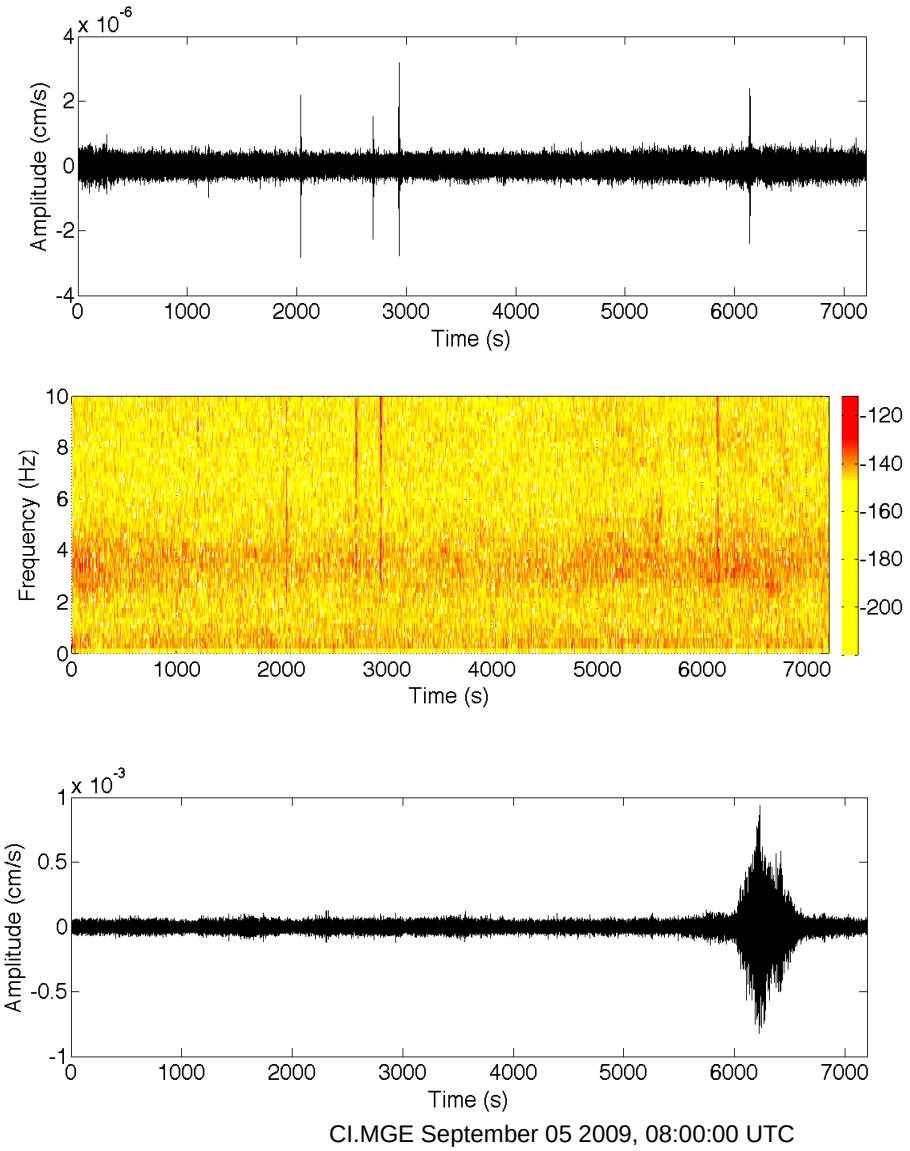

Figure 14. (a, top) North component seismogram recorded at station B084 during the first 7000 s shown in Figure 8. (b, middle) Spectrogram showing a persistent 3-4 Hz hum (red band). Colorbar units are arbitrary. (c, bottom) Seismogram recorded at MGE during the same time interval. During the first hour no trains were running between stations DEV and NSS2, while in the second hour there is one train northbound..

Agnew (2012) identified low-amplitude signals recorded on borehole instruments in

Anza and concluded that they were generated by truck traffic through the Coachella Valley, primarily along the I-10 corridor. *Agnew* (2012) rules out freight trains as the source of these signals based on his observation that noise on the borehole stations is significantly lower on Sundays than other days of the week, whereas train activity, as detected by a laser strainmeter close to the train track (at Durmid Hill, near station CI.BAT), is sustained all week long.

Discussion and Conclusions

Vibrations from truck and train traffic along the Coachella Valley, a major transportation artery, appears to be the primary source of seismic noise at roughly 1-5 Hz in the Anza region. These signals are low-amplitude and difficult to distinguish in the time domain at the noisier surface stations, but are readily detected by dense arrays, and more clearly seen on Anza borehole instruments. Using borehole Anza stations as well as surface CISN stations along the Coachella Valley, we show that trains running along the Coachella Valley, in proximity to station MGE, generate vibrations that are associated with visually detectable transients at most of the borehole sites. We determined that the transients are associated with train traffic, while the sustained hum is associated with truck traffic. Both forms of seismic noise have similar frequency-domain signatures. It is not surprising that the natural period of the two are similar. Many freight cars carry shipping containers that are also hauled by big rigs. The overall size of freight cars and big rigs are moreover similar, although loaded freight cars can be significantly heavier (100 tons versus a maximum legal limit of 40 tons on most US highways). We thus conclude that both trains and trucks generate the predominate 2-5 Hz noise observed across the Anza array, with trains generating visually apparent transients with durations on the order of 20 minutes.

The transients are strong enough to generate correlated noise envelopes across the Anza borehole array within the 2 to 8 Hz frequency band, lasting a few tens of minutes (Figure 2). Moreover, the transients consist of near-repeats of highly similar short-duration waveforms (Figure 4), due to the localized nature of the sources (small size relative to wavelength). Because these features are similar to those of tectonic tremor signals, the train-induced signals can effectively masquerade as tectonic tremor. Thus were these signals identified using a tremor-detection approach designed based on characteristics of tremor observed elsewhere. The ubiquitous nature of the identified noise sources in the Coachella Valley is likely one of the reasons why tectonic tremor has been difficult to observe along the San Jacinto fault; the other possible reason being that perhaps it simply does not occur. In any case, our results place bounds on the capability to detect spontaneous tremors in southern California with current instrumentation and analysis techniques. Our characterization of the noise will be useful to develop tremor detection algorithms that are not fooled by cultural noise sources that have confounded traditional approaches.

Although analysis reveals a non-geophysical origin of the transient signals observed at

Anza, these abundant signals, which we have shown can be traced to identifiable (moving) sources, can be exploited to improve our shallow attenuation model for the region. The skin depth of the inferred high-frequency surface waves generated by trains is intermediate between the depths accessible by boreholes and the depth range over which conventional seismological investigations provide resolution. Preliminary calculations presented in this study reveal that Q increases more strongly with depth than suggested by more coarse models inferred from analysis of seismic data. Similar studies exploiting high-frequency ground motion induced by traffic could be undertaken in regions of low seismicity rate to complement the earthquake hazard assessment of critical facilities.

Data and Resources

All data analyzed for this study were downloaded from the Southern California Earthquake Data Center and the IRIS Data Management Center.

Bibliography

Agnew, D.C. (2012). Widespread anthropogenic seismic tremor: sources and effects, Rep. to Southern Calif. Earthq. Center.

Aki, K., M. Fehler, and S. Das (1977). Source mechanism of volcanic tremor: fluid-driven crack models and their application to 1963 Kilauea eruption*, J. Volc. And Geotherm. Res.* 2, 259-287, doi: 10.1016/0377-0273(77)90003-8.

Barbour, A.J. and D.C. Agnew (2012). Detection of seismic signals using seismometers and strainmeters, *Bull. Seism. Soc. Am.,* 6, 2484-2490. Doi: 10.1785/0120110298.

Berger, J., L.M. Baker, J.N. Brune, et al. (1984). The Anza array: a high-dynamic-range, broad-band, digitally radiotelemetered seismic array, *Bull. Seism. Soc. Am.* 74, 1469-1481.

Brown, J.R., G.C. Beroza, and D.R. Shelly (2008). An auto-correlation method to detect low frequency earthquakes within tremor, Geophys. Res. Lett., 35, doi: 10.1029/2008GL034560.

Fletcher, J.B., T. Fumal, H-P. Liu, and L.C. Carroll (1990). Near-surface velocities and attenuation at two boreholes near Anza, California, from logging data, *Bull. Seism. Soc. Am.* 80, 807-831.

Fletcher, J. B., Spudich, P., & Baker, L. M. (2006). Rupture propagation of the 2004 Parkfield, California, earthquake from observations at the UPSAR. *Bull. Seism. Soc. Am.*, *96*(4B), S129-S142.

Fletcher, J.B. and L.M. Baker (2010). Analysis of nonvolcanic tremor on the San

Andreas fault near Parkfield, CA, using U.S. Geological Survey Parkfield Seismic Array, *J. Geophys. Res.* 115, B10305, doi:10.1029/2010jb007511.

Frankel, A., S. Hough, P. Friberg, and R. Busby (1991). Observations of Loma Prieta aftershocks from a dense array in Sunnyvale, California, *Bull. Seism. Soc. Am.* 81, 1900-1922.

Fry, B., K. Chao, S. Bannister, et al. (2011). Deep tremor in New Zealand triggered by the 2010 Mw8.8 Chile earthquake, *Geophys. Res. Lett.* 38, art. L15306, doi: 10.1029/2011GL048319

Gomberg, J., J. L. Rubinstein, Z. Peng, K. C. Creager, J. E. Vidale, and P. Bodin (2008). Widespread Triggering of Nonvolcanic Tremor in California, *Science*, 319, 173, doi:10.1126/science.1149164

Hough, S.E. and J.G. Anderson (1988). High-frequency spectra observed at Anza, California: Implications for Q structure, *Bull. Seism. Soc. Am. 78,* 692-707.

Ide, S., D.R. Shelly, and G.C. Beroza (2007). Mechanism of deep low frequency earthquakes: further evidence that deep non-volcanic tremor is generated by shear slip on the plate interface, Geophys. Res. Lett. 34, DOI: 10.0129/2006GL028890

Nadeau, R.M. and D. Dolenc (2005). Nonvolcanic tremors deep beneath the San Andreas fault, Science 307, 389, doi: 10.1126/science.1107142

Obara, K. (2002). Nonvolcanic deep tremor associated with subduction in southwest Japan, Science 296, 1679-1681, doi:

Peng, Z. and K. Chao (2008). Non-volcanic tremor beneath the Central Range in Taiwan triggered by the 2001 Mw7.8 Kunlun earthquake, Geophys. J. Int. 175, 825-829, doi: 10.1111/j.1365-246X.2008.03886.x

Peng, Z., J.E. Vidale, A. Wech, et al. (2009) Remote triggering of tremor along the San Andreas fault in central California, J. Geophys. Res. 114, doi: 10.1029/2008JB006049

Sanders, C.O. and H. Kanamori (1984). A seismotectonic analysis of the Anza seismic gap, San Jacinto fault zone, southern California, J. Geophys. Res., 89, 5873-5890.

Shelly, D.R., G.C. Beroza, S. Ide, and S. Nakamula (2006). Low-frequency earthquakes in Shikoku, Japan, and their relationship to episodic tremor and slip, Nature 442, 188-191, doi: 10.1038/nature04931

Shelly, D.R., G.C. Beroza, and S. Ide (2007). Non-volcanic tremor and low-frequency earthquake swarms, Nature 446, 305-307, doi:10.1038/nature05666

Shelly, D.R. and J.L. Hardebeck (2010). Precise tremor source locations and amplitude variations along the lower-crustal central San Andreas fault, Geophys. Res. Lett. 37, doi: 10.1029/2010GL043672.

Wdowinski, S. (2009), Deep creep as a cause for the excess seismicity along the San Jacinto fault, Nature Geoscience, 2, 882–885, doi:10.1038/ngeo684.

Wech, A.G., C.M. Boese, T.A. Stern, and J. Townend (2012). Tectonic tremor and deep slow slip on the Alpine fault, Geophys. Res. Lett., 39, doi: 10.1029/2012GL051751

Wesnousky, S.G. (1994). The Gutenberg-Richter or characteristic earthquake distribution, which is it? Bull. Seism. Soc. Am. 84, 1940-1959.

Yang, W., E. Hauksson, and P.M. Shearer (2012). Computing a large refined catalog of focal mechanisms for southern California (1981-2010): Temporal stability of the style of faulting, Bull. Seism. Soc. Am. 102, 1179-1194, doi: 10.1785/0120110311